Central Ring Electrode for Trapping and Excitation/Detection in Fourier Transform Ion Cyclotron Resonance Mass Spectrometry

C. M. Ostrander, C R. Arkin, and David Laude
Department of Chemistry and Biochemistry, The University of Texas at Austin, Austin, Texas, USA

The use of a central trapping ring electrode for Fourier transform ion cyclotron resonance (FTICR) mass spectrometry is demonstrated. Ions are trapped with an oppositely biased static potential superimposed on both the excite and detect electrodes and maintained throughout the experiment, including the application of a dipolar rf excite waveform and the image current ion detection event. The use of a central trapping electrode for FTICR coupled with an open cell design retains the advantages of high ion throughput and gas conductance, while simplifying the electrode geometry and reducing the overall dimensions of the cell. This allows the central trapping electrode to be of utility in volume-limited vacuum chambers including FTICR instrument miniaturization. Presented here are the preliminary experimental results using the central trapping electrode as an FTICR cell in which the excitation and detection electrodes also create a trapping depression to constrain the *z*-axis motion of the ions. The cell overcomes the principle limitation of an earlier single trapping electrode design by producing a 91% effective potential well depth compared to 19% for the single trapping electrode and 33% for standard open cells. This allows the central trapping electrode configuration to achieve an order of magnitude improvement in ion capacity compared to more conventional open cell designs. (J Am Soc Mass Spectrom 2000, 12, 30–37) © 2000 American Society for Mass Spectrometry

The progress of Fourier transform ion cyclotron resonance (FTICR) [1, 2] mass spectrometry for use in conjunction with external ionization techniques such as electrospray ionization (ESI) [3, 4] and matrix assisted laser desorption/ionization (MALDI) [5] has spawned interest in alternative trapped-ion cell configurations [6]. Various electrode arrangements of cubic [7], orthorhombic [8, 9], cylindrical [10–13], hyperbolic [14–16], or multiple-electrode [17–20] configurations have been implemented to improve analytical figures of merit. For example, hyperbolic electrode cells were adapted to FTICR to maximize mass resolution by producing a nearly pure quadrupolar potential. Cubic cells were elongated to increase dynamic range while reducing space charge and radial electric field effects [21]. Grounded screens positioned between the trap electrodes and the excite/detect electrodes were used to reduce the radial electric field by up to two orders of magnitude [17]. Recently, ion traps have been "matrix shimmed" by segmenting the electrodes and implementing extensive capacitive networks to optimize the electric field potentials [22–24]. Each of these improvements in cell design has resulted in improved FTICR performance, but has come at the expense of increasing the complexity of the electrode configuration and the circuitry involved.

Variations on the traditional closed cell design do not address the current needs of external ion sources such as the difficulty in introducing a charged particle beam through a narrow conductance limit without charging or contaminating the trap electrodes, and the necessity of passing the ion current in close proximity to paramagnetic electrode materials [25]. Beu and Laude introduced the open geometry [26] trapped-ion cell for FTICR, which allowed for conventional mass analysis to be performed with the trap electrodes positioned parallel to excitation and detection electrodes in a collinear electrode geometry. The open cell has advantages of increased external ion injection efficiency, improved gas conductance in the cell, and reduced ion trajectory perturbations from ions that pass in proximity to paramagnetic electrode surfaces [27, 28]. FTICR performance is also enhanced due to the increased excitation field homogeneity because the excitation field does not terminate as abruptly on the trap electrodes compared to orthogonally positioned electrodes. Increased flexibility in the open cell design permits capacitive coupling of the excitation electrodes to the trap electrodes to further improve excitation field uniformity and reduce mass-dependent axial ejection [29].

The typical FTICR open trapped-ion cell consists of three collinear cylindrical rings. As with closed

Address reprint requests to Dr. David Laude, Department of Chemistry & Biochemistry, University of Texas at Austin, Austin, Texas 78712. E-mail: dalaude@mail.utexas.edu

1044-0305/00/$20.00
PII S1044-0305(00)00193-8

Received April 27, 2000
Revised August 14, 2000
Accepted August 14, 2000

trapped-ion cells, the potential well is formed by using the two outside rings as trapping electrodes to which a voltage of the same polarity of the ions to be trapped is applied. The center ring electrode is segmented into four equal parts at 0, 90, 180, and 270 deg for excitation and detection. As an alternative open cell design, Vartanian and Laude demonstrated a single annular trap electrode located at the center of the excitation and detections electrodes that creates a trapping potential well when a static potential of opposite polarity of the charged ion is applied [30]. With this single annular trapping electrode, FTICR performance is improved by reducing the radial electric field throughout a significant portion of the trapping volume. This single trapping electrode geometry is an example of the increased flexibility in cell design made possible with the open cell configuration.

Central Trapping Electrode

To be presented in this work is the generalization of Vartanian's single trapping electrode, in which the central electrodes, usually reserved for excitation and detection, are also used to create the trapping well that constrains the *z*-axis ion motion. Shown in Figure 1a is a standard closed cylindrical cell in which the trapping potential well for positive ions is typically produced by applying positive voltages to the outer trapping electrodes. However, it is also possible to create a trapping well by applying a negative voltage to the center electrodes. This was first demonstrated with Vartanian's single trapping electrode, which is shown in Figure 1b. An obvious criticism of Vartanian's single trapping electrode is interference between the applied trapping field and the excitation and detection fields. The central trapping electrode design, shown in Figure 1c, eliminates the need for the annular trapping ring by superimposing the dc trapping voltage on the excite and detect electrodes. In both Figure 1b, and c, the potential difference is created with the grounded vacuum chamber.

In this new work, the central trapping electrode offers a significant improvement on the limitations of the single trapping electrode. As with the single trapping electrode, the central trapping electrode is segmented into excitation and detection electrodes. However, a trapping well is achieved not with a distinct annular ring electrode, but instead by applying a static potential to both the excite and detect electrodes that is maintained throughout the application of a dipolar rf excite waveform as well as the image current ion detection. The use of a central trapping electrode for FTICR should exhibit open cell advantages including high ion throughput and gas conductance while minimizing elaborate electrode geometry and size. Maintaining standard open cell performance at a reduced electrode size offers the opportunity for performing FTICR mass analysis in space limited instruments. Finally, because the trapping dimension extends over the entire range of the excitation and detection field, the trapping well depth and ion capacity should increase. This latter benefit was previously demonstrated utilizing the central trapping electrode as an ion accumulation cell for increasing sensitivity and duty-cycle performance in a volume-limited region on an internal bore LC-ESI/FTICR mass spectrometry [31].

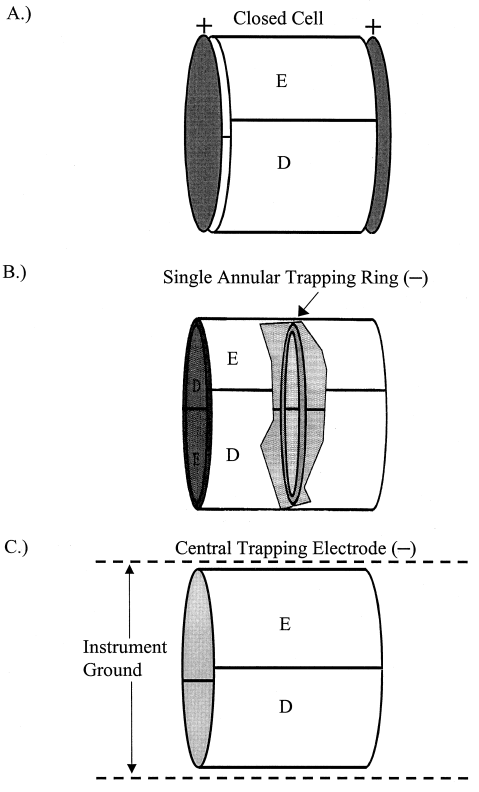

Figure 1. (**a**) The standard three electrode closed cylindrical cell. (**b**) Diagram of the single trapping electrode cell. The annular trap electrode is positioned in the center of the excitation and detection region. The two sets of excitation and detection electrodes are employed as in the conventional FTICR cell. (**c**) The central trapping electrode cell. The central trapping electrode only utilizes the excite and detect electrodes. The dc trapping potential is superimposed on the excite and detect electrodes.

Presented here are the initial experimental results demonstrating that the FTICR experiment is possible when the excitation and detection electrodes are also used to create the *z*-axis trapping depression.

Experimental

FTICR performance is evaluated for the central trapping electrode and the standard open cylindrical cell. As will be demonstrated, the standard open cell can be electrically configured to provide a close approximation of the fields created by the central trapping electrode in a confined volume vacuum chamber. This electrical reconfiguration is employed in these feasibility studies.

The standard open cell consists of three collinear ring electrodes. The center ring electrode is segmented into

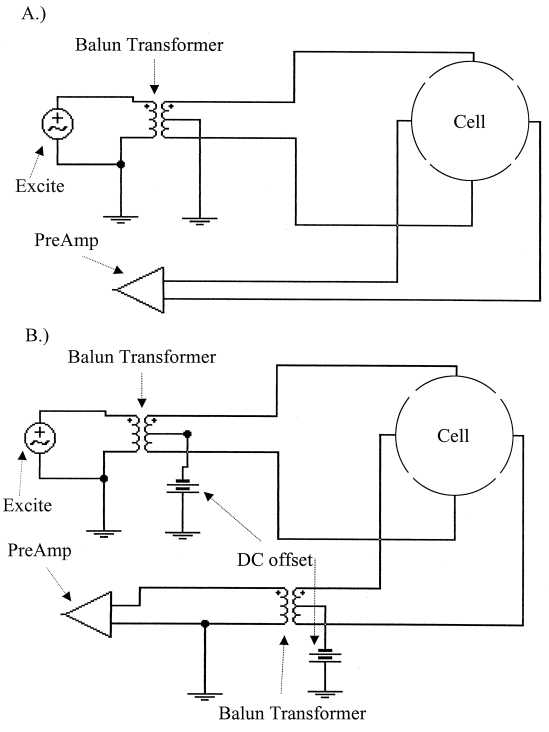

Figure 2. A diagram of cell connections and wiring for (**a**) standard open cell and (**b**) central trapping electrode. The superimposed dc offset is applied to the center tap of the balun transformer.

four parts at 0, 90, 180, and 270 deg for the excite/detect electrode. The overall cell dimensions of the standard open cell are 50 mm in diameter and 133 mm in length including a 45 mm length for the excite/detect ring electrode, a 42 mm length for each of the trapping ring electrodes, and two 2 mm air gaps. The cell connections and circuit diagram are shown in Figure 2a. The excitation waveform is sent trough a balun transformer generating the two identical (180 degrees out of phase) dipolar signals for the excite electrodes, and the detect electrodes are connected directly to a preamp.

As previously mentioned, for the experimental data presented, the same cell is utilized to evaluate the central trapping electrode in comparison to the standard open cell. However, the central trapping electrode only uses the central excite/detect electrodes of the standard open cell. The trapping electrodes are held at instrument ground, and as will be demonstrated, have a negligible effect compared to vacuum chamber ground. Ions are trapped by superimposing the dc trapping potential on the excitation and detection electrodes while the trapping ring electrodes are maintained at instrument ground. Maintaining the standard open cell trapping rings at instrument ground effectively mimics the central trapping electrode cell in a volume-limited region without compromising the ability to compare the experimental performance to that of the standard open cell.

The overall dimensions of the central trapping cell are 50 mm in diameter and 45 mm in length. The cell connections and circuit diagram are shown in Figure 2b. For positive ion detection, a negative static trapping potential is applied to the excite electrodes of the central trapping ring electrode via the center tap of a North Hills (Syosset, NY) wide-band (10 kHz–15 MHz) balun transformer (model 0902BB). The negative static trapping potential is applied to the detect electrodes of the central trapping ring electrode via an additional balun transformer positioned between the preamp and the detect electrode feeds.

Experiments were performed using electron ionization (EI) on a 3 tesla FTICR mass spectrometer [31, 32]. A typical experimental sequence involves trapping ions by applying a negative potential (-1 to -10 V) to the central trapping electrode during the entire pulse sequence starting with a standard EI ionization (55 eV, 1.0 ms) event and a 0.5 s axial cooling delay. The excitation event was performed with either a broadband dipolar chirp or a single frequency excite. Following a 500 μs postexcitation delay, a direct mode detection event was performed. All samples were purchased from Sigma (St. Louis, MO) and introduced through a high precision leak valve (Varian model 951-5106, Lexington, MA). Data acquisition and processing were performed with a Midas Data Station running version 3 software [33]. The spectra presented here are baseline corrected, Hanning apodized, and zero filled once before Fourier transformation. All FTICR data analyses were performed using the ICR-2LS data analysis package [34].

For the simulations performed, the central trapping electrode, the single trapping electrode, the cubic cell, and the standard open cell has an aspect ratio of 1 and a diameter of 50 mm. In addition, simulations were performed on the elongated open cell, aspect ratio 2, for comparison. SIMION [35] 3D version 6.0 (D. A. Dahl, Idaho National Engineering Labs, Idaho Falls, ID) modeling was utilized to calculate the centerline trapping potential wells. The trapping profiles were generated by trajecting a 100 eV ion down the centerline of the cell to determine the potential along the z axis. Potential arrays are redefined at an iteration limit of 20 and a convergence objective of 5.0×10^{-3}. For all simulations, the applied trapping potential is -10 V for the central trapping configuration and 10 V for the standard configuration. When simulating the central trapping electrode configuration, the vacuum chamber dimensions were fixed at double the cell radius and four times the cell length.

Results/Discussion

To properly simulate and evaluate the trapping environment of trapped ion cells, the aspect ratio or relative dimensions of the cell must be defined. The aspect ratio for closed cells is simply defined as the ratio of the cell length c_e, which is the distance between the parallel trapping electrodes, and the cell width w, which is the

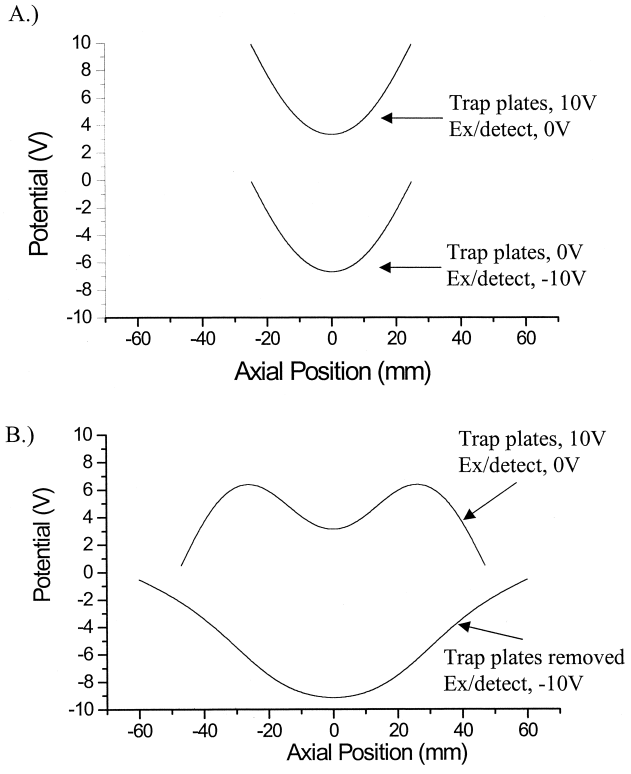

Figure 3. SIMION plots comparing the effects of utilizing the excite/detect electrodes to create the trapping environment for (**a**) the closed cubic cell aspect ratio 1 and (**b**) the open cylindrical cell aspect ratio 1. Note the increased trapping potential well for the open cell and the removal of the positive electrostatic barrier for both cells.

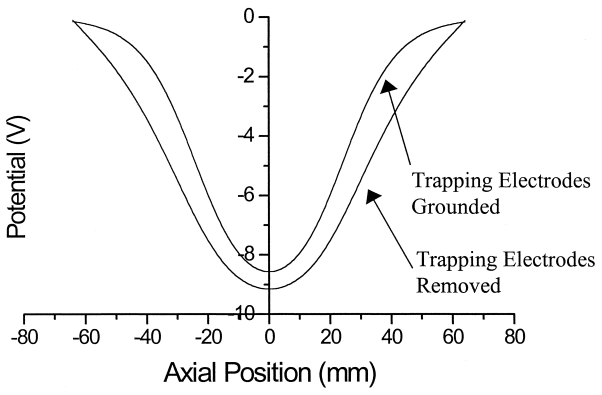

Figure 4. SIMION was used to model our system to evaluate the trapping potential wells produced when the excite/detect electrodes of a standard open cylindrical cell are negatively biased (−10 V applied) and the trapping electrodes are either grounded or removed. The standard open cell trapping electrodes are grounded to simulate a volume-limited vacuum chamber and preserve the ability to experimentally compare results to that of the standard open cell.

diameter of the cell. Thus the cubic cell in which c_e = w has an aspect ratio of 1. This method would apply to all closed cells as well as the central trapping electrode and single trapping electrode cells. However, in open cells the trapping electrodes c_t extend significantly beyond the length of the central excite/detect electrodes. For simplicity, the gap distance is considered negligible and the open cell length is $c_e + c_t$, with the cell boundaries near midpoints of the trapping electrodes. Thus the open cell analog to the cubic cell of aspect ratio 1 is formed with dimensions of $c_t = c_e = 0.5\ w$ and the open cell analog to an elongated closed cell of aspect ratio 2 is formed with dimensions of $c_t = c_e = w$.

Cell Theory

Prior to experimentally evaluating the central trapping electrode, SIMION was used to determine the effects of the trapping environment when the excite and detect electrodes are used to create the trapping well. As a first example, the traditional closed cubic cell, aspect ratio 1, trapping depression is evaluated. Figure 3a contrasts the trapping potential depressions of a closed cubic cell when +10 V is applied to the trapping electrodes and the excite/detect electrodes are held at ground compared to applying −10 V to the excite/detect electrodes with the trapping electrodes grounded. When utilizing a closed cell, the vacuum chamber geometry and the effect of instrument ground is not significant. Therefore, the shape of the trapping potential well is identical producing a well depth of 6.6 V for both configurations.

In Figure 3b, the trapping environment for the open cylindrical cell, aspect ratio 1, is evaluated. Again, the conventional open trapping configuration is contrasted with the central trapping electrode configuration. Figure 3b demonstrates that the trapping potential wells produced are more effective when the excite/detect electrodes are used for trapping in the open cell configuration. Utilizing the excite and detect electrodes for creating the trapping depression creates a 9.1 V potential well compared to a 3.3 V potential well for the standard configuration. This allows for creating trapping depressions greater than that of the closed cell while maintaining the benefits of the open cell configuration. It should be realized that when using the central trapping electrode open cell configuration to create the trapping region, the magnitude of the trapping potential well is dependent on the proximity of instrument ground, making trapping electrodes unnecessary in a confined volume region.

Cell Design

To validate the grounding of the standard open cell trapping electrodes to simulate instrument ground for the central trapping electrode, SIMION was used to model the vacuum chamber and cell configuration. The trapping potential wells were calculated when utilizing the excite/detect electrodes for trapping while grounding the existing trapping electrodes compared to removing them entirely. Figure 4 demonstrates the rela-

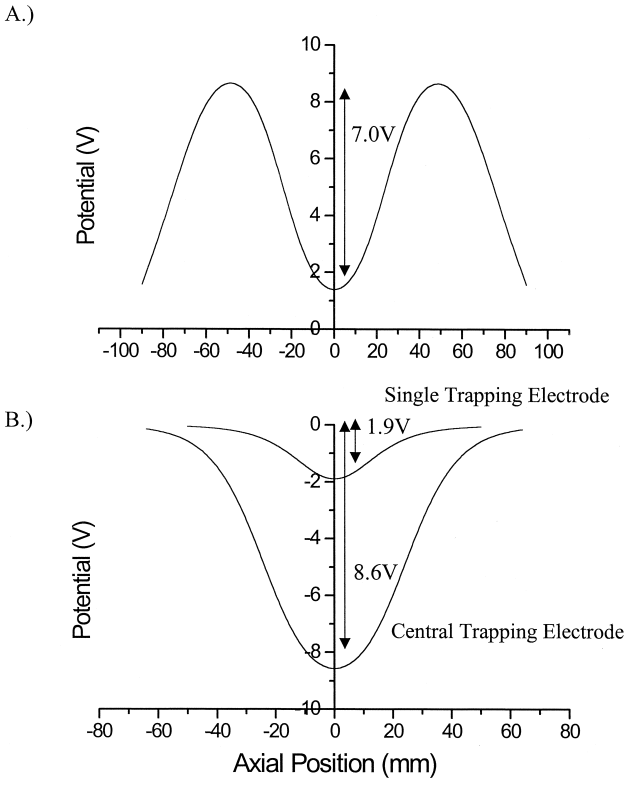

Figure 5. SIMION plots of the trapping potentials along the cell centerline for the experimental conditions of (**a**) the standard open cell aspect ratio 2 and (**b**) the central trapping electrode and single trapping electrode aspect ratio 1. The central trapping electrode has an 86% effective well depth compared to 19% for single trapping electrode and 33% for the standard open cell.

tively similar trapping environments for the two configurations. The maximum well depth is within 7% and the well width is within 15% at half magnitude. Grounding the existing trapping electrodes actually results in an overall decrease in size of the trapping potential when compared to the grounded vacuum chamber. However, as the size of the vacuum chamber decreases, the ratio of the two potential wells should approach unity. It is important to note that the effectiveness of the central trapping electrode is dependent on ground plane proximity, limiting the utility of the cell to the confined volume regions. Fortunately, this limitation is complementary to the significant reduction in cell length achieved by the central trapping electrode, making the cell ideal for volume-limited applications.

The ability of the central trapping electrode for ion trapping is dependent on the formation of a potential well to constrain the *z*-axis motion of the ions. To obtain a quantitative understanding of the magnitude of the trapping potential well, SIMION is used to create the centerline trapping potential profiles in Figure 5 for comparison to the elongated open cylindrical cell and the single trapping electrode. For these simulations, the experimental conditions are modeled in which the open cell configuration retains the advantages of an elongated cell with aspect ratio 2, and the single trapping electrode and central trapping electrode posses an aspect ratio of 1. In addition, for the central trapping electrode simulations the standard open cell trapping electrodes are grounded to simulate conditions in a confined volume for which the cell would be advantageous. The central trapping electrode differs from the single trapping electrode and the standard open cell in that a deeper trapping well is achieved for a particular applied voltage. For example, a +10 V applied potential creates a 6.9 V trapping well for the standard open cell, and a −10 V applied potential creates a 1.9 V trapping well for the single trapping electrode and a 8.6 V trapping well for the central trapping electrode. Consequently, a smaller applied potential is required to achieve the desired well depth for the central trapping electrode. The increase in the effective potential well of the standard open cell in Figure 3 is a result of the increased aspect ratio in Figure 5. The advantage of an increased effective potential well of the central trapping electrode is particularly magnified when compared to the single trapping electrode, which was made as narrow as possible to minimize effects of excitation and detection, and consequently generated shallow trapping wells. In addition, the central trapping electrode creates a wider potential well providing the opportunity for increased trapping dynamic range at optimized applied potentials. The full-width at half-magnitude is 70 mm for the central trapping electrode potential well compared to 50 mm for the standard open cell.

Cell Performance

As mentioned earlier, the primary limitation of the single trapping electrode was the interference of the annular trapping electrode with the excitation and detection fields. This interference ultimately limited the overall performance of the cell and was manifested as signal reduction and peak broadening due to the dephasing of the ion packet that occurred if the ions traveled in close proximity to the annular trapping ring. As a result, for the single trapping electrode geometry the ions were only capable of being accelerated to 60% of the cell radius before the annular trapping ring distorted the radial trajectory of the ions [30]. Figure 6a demonstrates that the central trapping electrode configuration does not exhibit this limitation, and is capable of excitation to the full extent of the cell radius [36].

An additional negative consequence of the need to minimize ion signal interference from the annular trapping ring in the single trapping electrode was that the trapping ring itself was made as narrow as possible. Consequently, the trapping wells were necessarily shallow, thus limiting the ion capacity of the cell. Figure 5 demonstrates the increased potential well depth of the central trapping electrode compared to both the single trapping electrode and the standard open cell resulting in an increased ion capacity. The improved ion capacity for the central trapping electrode compared to the

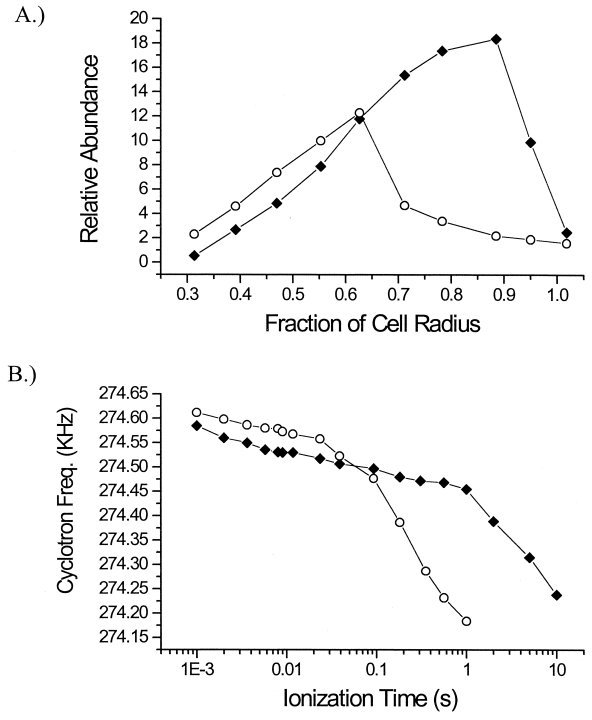

Figure 6. (**a**) Excitation profile for pentafluorobenzene (*m/z* 168) at increasing fraction of cell radius for the central trapping electrode compared to the single trapping electrode. Signal intensity deteriorates at 90% cell radius for the central trapping electrode (filled diamond) and 60% for the single trapping electrode (open circle). (**b**) Data plot of increasing ionization time (pentafluorobenzene) for the central trapping electrode (filled diamond) and the standard open cell (open circle). The data reveals the increased ion capacity for the central trapping electrode.

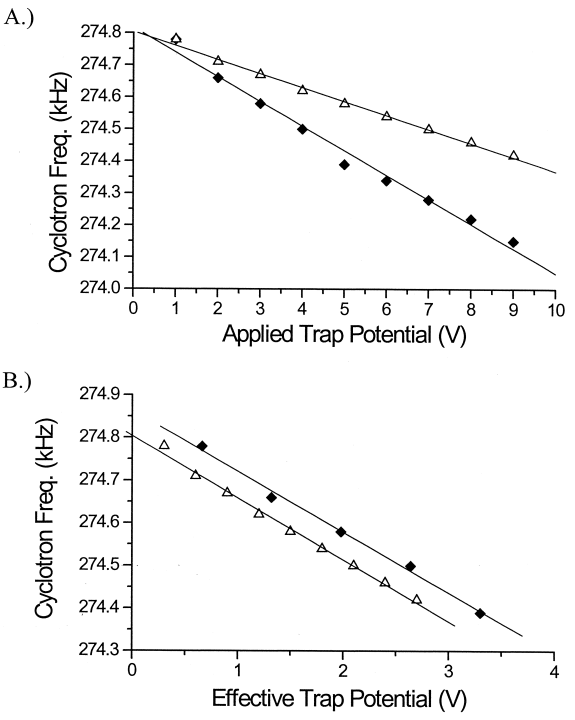

Figure 7. (**a**) Data plot demonstrating the negative shift in measured cyclotron frequency as radial electric field increases with increasing trap potential for pentafluorobenzene (*m/z* 168), central trapping electrode (filled diamond), standard open cell (open triangle). Slopes are −75 Hz/V for the central trapping electrode and −45 Hz/V for the standard open cell. (**b**) Same plot as (**a**) corrected for the effective trapping potential. The slope is the same for both cells, −140 Hz/V.

standard open cell is illustrated in Figure 6b, which shows the analyte ionization time threshold for linear response is about an order of magnitude longer for the central trapping electrode cell configuration. Deviations in the linearity of the cyclotron frequency shifts (>0.01%) occur at an ionization time of 1.0 s for the central trapping electrode and 0.1 s for the standard open cell. In comparison to the single trapping electrode, this improvement in ion capacity should be magnified as a result of the relatively shallow trapping potential well produced by that cell.

In all trapped ion cells, the radial electric field component of the trapping field is responsible for frequency shifts in the observed cyclotron frequency. The magnitude of the shift is an important measure of cell performance. As shown in Figure 7a, the trapping potential dependent frequency shift of the central trapping electrode is greater than that of the standard open cell, suggesting an increased radial electric field at equal trapping potentials. Specifically, the central trapping electrode produces a frequency shift at the rate of −75 Hz/V compared to −45 Hz/V for the standard open cell. However, this effect is mitigated because of the greater well depth produced by the central trapping electrode at similar trapping potentials. This is demonstrated by comparing the cyclotron frequency shifts for the central trapping electrode and the standard open cell to the effective potential well as shown in Figure 7b. Both cells produce a frequency shift of about −140 Hz/V when considering the effective potential well.

An additional aspect of trapped ion cells is low mass discrimination as a result of axial ejection. Different molecular weight ion abundances were evaluated to investigate the extent of mass dependent axial ejection using the central trapping electrode and the standard open cell. The data presented in Figure 8 demonstrates the reduction in low mass ion abundance due to axial ejection in both the central trapping electrode (Figure 8a) and the standard open cell (Figure 8b). Although both cell configurations exhibit low mass discrimination, the reduction in low mass abundance is slightly greater for the central trapping electrode. One possible explanation is that the axial extent of the ions is greater for the central trapping electrode as a result of the wider trapping wells produced.

Conclusions

The central trapping electrode achieves many of the desired characteristics for FTICR mass spectrometry

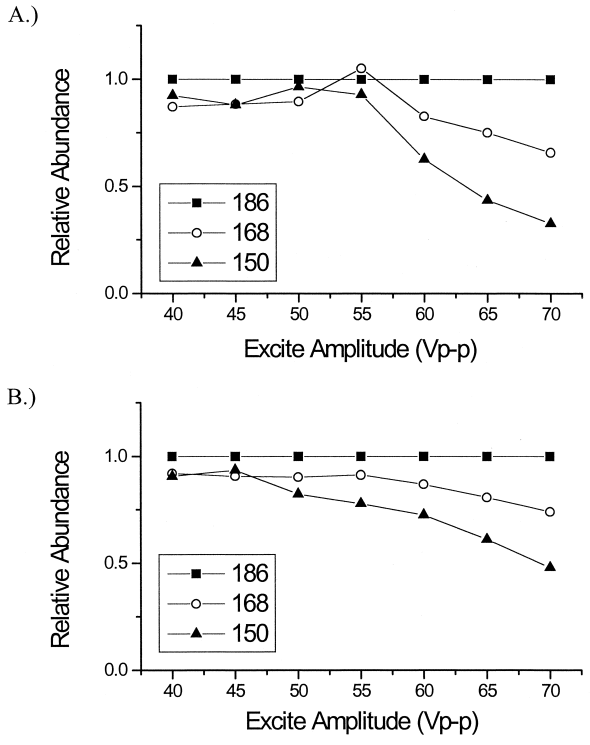

Figure 8. Relative abundances of tetrafluorobenzene (m/z = 150), pentafluorobenzene (m/z = 168), and hexafluorobenzene (m/z = 186) ions with constant applied trapping voltage as the excite voltage amplitude is increased. The central trapping electrode is shown in (**a**), and the standard open cell in (**b**). As a result of the wider trapping potential well, the axial extent of the ions is greater resulting in a slight increase in low mass discrimination for the central trapping electrode.

while using only a single segmented ring electrode. Advantages include a reduction in cell size and electrode complexity, providing the opportunity for utilizing the central trapping electrode in volume-limited vacuum chambers. Utilizing the central trapping ring electrode provides open cell advantages of high ion throughput and gas conductance while maintaining the performance of standard three electrode open cells. In addition, with equivalent aspect ratios, the central trapping electrode produces a well depth at 91% of applied potential compared to 33% for the standard open cell and 19% for the single trapping electrode. The increased trapping well magnitude and efficiency allow for an order of magnitude improvement in ion capacity for the central trapping electrode, overcoming the primary limitation of the single trapping electrode and minimizing coulomb effects. Finally, the central trapping electrode cell is capable of accelerating ions to the full extent of the cell radius, whereas the single trapping electrode is limited to only 60% of the cell radius.

Future work will concentrate on exploiting the use of the central trapping FTICR cell for externally generated ions. In addition, research will continue in utilizing the central trapping electrode as an accumulation cell in a volume-limited dual cell LC-ESI/FTICR. The central trapping electrode accumulation cell will be used to perform ion selection or dissociation techniques using various radial excitation events prior to transfer to the analyzer cell.

References

1. Comisarow, M. B.; Marshall, A. G. *Chem. Phys. Lett.* **1974,** *25*, 282–283.
2. Comisarow, M. B. *J. Chem. Phys.* **1978,** *69*, 4097–4104.
3. Smith, R. D.; Loo, J. A.; Ogorzalek Loo, R. R.; Busman, M.; Udseth, H. R. *Mass Spectrom. Rev.* **1991,** *10*, 359–451.
4. Fenn, J. B.; Mann, M.; Meng, C. K.; Wong, S. F. *Mass Spectrom. Rev.* **1990,** *9*, 37–70.
5. Hillenkamp, F.; Karas, M.; Beavis, R. C.; Chait, B. T. *Anal. Chem.* **1991,** *63*, 1193A–1203A.
6. Vartanian, V. H.; Anderson, J. S.; Laude, D. A. *Mass Spectrom. Rev.* **1995,** *14*, 1–19.
7. Comisarow, M. B. *Int. J. Mass Spectrom. Ion Phys.* **1981,** *37*, 251–257.
8. McIver, R. T., Jr. *Rev. Sci. Instrum.* **1970,** *41*, 555–558.
9. Hunter, R. L.; Sherman, M. G.; McIver, R. T., Jr. *Int. J. Mass Spectrom. Ion Phys.* **1983,** *50*, 259–274.
10. Lee, S. H.; Wanczek, K.-P.; Hartmann, H. *Adv. Mass Spectrom.* **1980,** *8B*, 1645–1649.
11. Kofel, P.; Allemann, M.; Kellerhals, H.; Wanczek, K. P. *Int. J. Mass Spectrom. Ion Processes* **1986,** *74*, 1–12.
12. Gabrielse, G.; Mackintosh, F. C. *Int. J. Mass Spectrom. Ion Processes* **1984,** *57*, 1–17.
13. Schweikhard, L.; Lindinger, M.; Kluge, H.-J. *Rev. Sci. Instrum.* **1990,** *61*, 1055–1058.
14. Rempel, D. L.; Ledford, E. B., Jr.; Huang, S. K.; Gross, M. L. *Anal. Chem.* **1987,** *59*, 2527–2532.
15. Brown, L. S.; Gabrielse, G. *Rev. Mod. Phys.* **1986,** *58*, 233–311.
16. Schweikhard, L.; Lindinger, M.; Kluge, H.-J. *Int. J. Mass Spectrom. Ion Processes* **1990,** *98*, 25–33.
17. Wang, M.; Marshall, A. G. *Anal. Chem.* **1990,** *62*, 515–520.
18. Wang, M.; Marshall, A. G. *Anal. Chem.* **1989,** *61*, 1288–1293.
19. Hanson, C. D.; Castro, M. E.; Kerley, E. L.; Russell, D. H. *Anal. Chem.* **1990,** *62*, 520–526.
20. Jacoby, C. B.; Holliman, C. L.; Rempel, D. L.; Gross, M. L. *J. Am. Soc. Mass Spectrom.* **1993,** *4*, 186–189.
21. Jeffries, J. B.; Barlow, S. E.; Dunn, G. H. *Int. J. Mass Spectrom. Ion Processes* **1983,** *54*, 169–187.
22. Jackson, G. S.; White, F. M.; Guan, S.; Marshall, A. G. *J. Am. Soc. Mass Spectrom.* **1999,** *10*, 759–769.
23. Grosshans, P. B.; Chen, R.; Marshall, A. G. *Int. J. Mass Spectrom. Ion Processes* **1994,** *139*, 169–189.
24. Caravatti, P.; Allemann, M. *Org. Mass Spectrom.* **1991,** *26*, 514–518.
25. Kerley, E. L.; Russell, D. H. *Anal. Chem.* **1989,** *61*, 53–57.
26. Beu, S. C.; Laude, D. A., Jr. *Int. J. Mass Spectrom. Ion Processes* **1992,** *112*, 215–230.
27. Marto, J. A.; Guan, S.; Marshall, A. G. *Rapid Commun. Mass Spectrom.* **1994,** *8*, 615–620.
28. Beu, S. C.; Senko, M. W.; Quinn, J. P.; Wampler, F. M., III; McLafferty, F. W. *J. Am. Soc. Mass Spectrom.* **1993,** *4*, 557–565.
29. Beu, S. C.; Laude, D. A. *Anal. Chem.* **1992,** *64*, 177–180.
30. Vartanian, V. H.; Laude, D. A. *J. Am. Soc. Mass Spectrom.* **1995,** *6*, 812–821.
31. Ostrander, C. M.; Arkin, C.; Laude, D. A. *J. Am. Soc. Mass. Spectrom.* **2000,** *11*, 592–595.
32. Harper, C. J.; Ostrander, C. M.; Schmidt, E. G.; Drader, J. J.; Laude, D. A. *Proceedings of the 45th ASMS Conference on Mass Spectrometry and Allied Topics*; Palm Springs, California, 1–5 June 1997; p 394.

33. Senko, M. W.; Canterbury, J. D.; Guan, S.; Marshall, A. G. *Rapid Commun. Mass Spectrom.* **1996,** *10*, 1839–1844.
34. Anderson, G.; Bruce, J. ICR-2LS, version 2.20.62; Pacific Northwest National Laboratories.
35. Dahl, D. A.; Delmore, J. E. Idaho National Engineering Laboratory, P. O. Box 2726, Idaho Falls, ID 83403, 1988.
36. Marshall, A. G.; Hendrickson, C. L.; Jackson, G. S. *Mass Spectrom. Rev.* **1998,** *17*, 1–35.